ELSEVIER

Comput. Methods Appl. Mech. Engrg. 1926 (1999) 413–420

Computer methods in applied mechanics and engineering

www.elsevier.com/locate/cma

Spectra and pseudospectra for pipe Poiseuille flow

Anne E. Trefethen[a,*], Lloyd N. Trefethen[b], Peter J. Schmid[c]

[a]*The Numerical Algorithms Group Ltd., Wilkinson House, Jordan Hill Road, Oxford OX2 8DR, UK*
[b]*Oxford University Computing Laboratory, Wolfson Building, Parks Road, Oxford OX1 3QD, UK*
[c]*Department of Applied Mathematics, University of Washington, Seattle, WA 98195, USA*

Received 22 December 1997

Abstract

Numerically computed spectra and pseudospectra are presented for the linear operator that governs the temporal evolution of infinitesimal perturbations of laminar flow in an infinite circular pipe at Reynolds numbers 1000, 3000 and 10 000. The spectra lie strictly inside the stable complex half-plane, but the pseudospectra protrude significantly into the unstable half-plane, reflecting the large linear transient growth that certain perturbations may excite.

1. Introduction

Fluid flow through a pipe at high Reynolds number invariably becomes turbulent, even though a linear analysis shows that the laminar flow is stable to infinitesimal perturbations [9,14,20,21]. In this report we present results of large-scale computations via hybrid Chebyshev spectral collocation methods designed to shed light on this phenomenon of subcritical transition to turbulence. Specifically, we present plots of spectra and pseudospectra of the linear operator that governs the temporal evolution of infinitesimal perturbations of pipe Poiseuille flows at Reynolds numbers 1000, 3000 and 10 000. In the laboratory, transition to turbulence typically takes place around $R = 2000$, though laminar flows have been maintained under special circumstances at Reynolds numbers more than fifty times higher than this.

The context of this work is a development that has taken place in the last ten years in the field of hydrodynamic stability: the recognition that the natural transition to turbulence of certain canonical shear flows is dominated by effects that are linear but non-modal, that is, unrelated to eigenvalues and eigenmodes. The roots of this kind of analysis go back to Rayleigh and Orr, and more recent related contributions include those of Alfredsson, Benney, Bergström, Breuer, Criminale, Ellingsen, Gebhardt, Grossmann, Gustavsson, Haritonidis, Hultgren, Ioannou, Klingmann, Landahl, Mayer, Morkovin, O'Sullivan, Palm, Reshotko, Tumin, Waleffe and Zikanov, among others. The new point of view came to the fore in four papers published a few years ago:

Boberg and Brosa (1988): [4]
Butler and Farrell (1992): [6]
Reddy and Henningson (1993): [19]
Trefethen, Trefethen, Reddy and Driscoll (1993): [24]

The present report amounts to an extension of our earlier work [24], which dealt with plane Couette and Poiseuille flows, to the case of pipe Poiseuille flow. We do not give a full-scale discussion, but assume that the

* Corresponding author. E-mail: anne@nag.co.uk

0045-7825/99/$ – see front matter
PII: S0045-7825(98)00364-8

reader is familiar with [24]. We also hope the reader is familiar with [4], [6] and [19]. In particular, the paper [4] by Boberg and Brosa is a remarkable one, also concerned with the present problem of pipe Poiseuille flow. Unfortunately, the authors of [6], [19] and [24] appear to have been unaware of [4] at the time of writing. Other contributions to the linear, non-modal analysis of the pipe Poiseuille problem include [3], [16], [18], [22] and [26].

2. The operator $\mathscr{L}$

Consider the flow of an incompressible Newtonian fluid with kinematic viscosity ν through an infinite circular pipe of radius a, with cylindrical coordinates x (longitudinal), r (radial), and θ (angular). One solution to the Navier–Stokes equations for such a flow is the laminar velocity profile

$$u_0 = u_0(r) = V\hat{x}\left(1 - \frac{r^2}{a^2}\right), \tag{1}$$

where V is an arbitrary constant and $\hat{x}$ denotes the unit vector in the x direction. We define the Reynolds number for this flow to be $R = aV/\nu$. In the study of hydrodynamic stability, our concern is the evolution of a small perturbation of this laminar flow, which we write as

$$u_0 + u = u_0(r) + u(x, r, \theta, t)\,. \tag{2}$$

If u is infinitesimal, its evolution is governed by a linear equation

$$\frac{\mathrm{d}u}{\mathrm{d}t}(t) = \mathscr{L}u(t) \tag{3}$$

for some linear operator $\mathscr{L}$. It is the properties of this linearized Navier–Stokes operator $\mathscr{L}$ that we investigate in this report. The norm $\|\cdot\|$ that we use for defining the pseudospectra of $\mathscr{L}$ and in connection with quantities such as $\|e^{t\mathscr{L}}\|$ is the energy norm, equal to an appropriately scaled 2-norm, as in previous works in this area.

The problem under study can be simplified by Fourier transformation in two directions. Since the x variable is unbounded, its dual variable is an arbitrary real number, which we denote by $\alpha \in \mathbb{R}$. Since the θ variable is 2π-periodic, its dual variable is an integer, which we denote by $n \in \mathbb{Z}$. Conventionally, most treatments of the pipe Poiseuille problem work within the context of these two Fourier variables. Here, however, following [24], although our computations make use of the Fourier reduction, the results we ultimately plot pertain to the untransformed problem. Thus, the spectra and pseudospectra we present correspond to $\mathscr{L}$, not $\mathscr{L}_{\alpha,n}$. Such a procedure has the disadvantage that effects of different Fourier components may be confused, but the advantage that one sees the whole problem at once rather than just one component that may or may not be dominant.

3. Spectra

Figs. 1(a), 2(a) and 3(a) show the spectrum $\Lambda(\mathscr{L})$ for $R = 1000$, 3000 and 10 000. So far as we are aware, although spectra have been calculated previously for operators $\mathscr{L}_{\alpha,n}$ corresponding to particular choices of Fourier parameters [8,9,22], plots such as these for the full operator $\mathscr{L}$ have not appeared before. (Our Fig. 2 was presented previously as Fig. 10 in the survey paper [23].)

For each R, $\Lambda(\mathscr{L})$ consists of a collection of curves in the complex left half-plane. (Note that to bring out the effects of greatest interest, we have scaled the real and imaginary parts differently by a factor of ten.) Each curve can be thought of as parametrized by the Fourier variable α, and the various curves correspond to various values of n, with infinitely many curves for each value of n, though only finitely many in any given part of the plane.

To clarify how it is that various values of n combine to give the full spectrum, Fig. 4 is a breakdown of the case $R = 1000$ for $n = 0, 1, 2, 3, 4, 5$. (Here and below we assume $n \geqslant 0$, since the contributions to the spectrum and the pseudospectra for n and $-n$ are the same.) One sees that the value $n = 1$ is dominant, and this is true also of other Reynolds numbers. As n increases, the spectrum sinks into the left half-plane. In the portion of the plane shown in our figures, the values of n that contribute to the picture are $n \leqslant 6$ for $R = 1000$, $n \leqslant 12$ for $R = 3000$ and $n \leqslant 27$ for $R = 10\,000$.

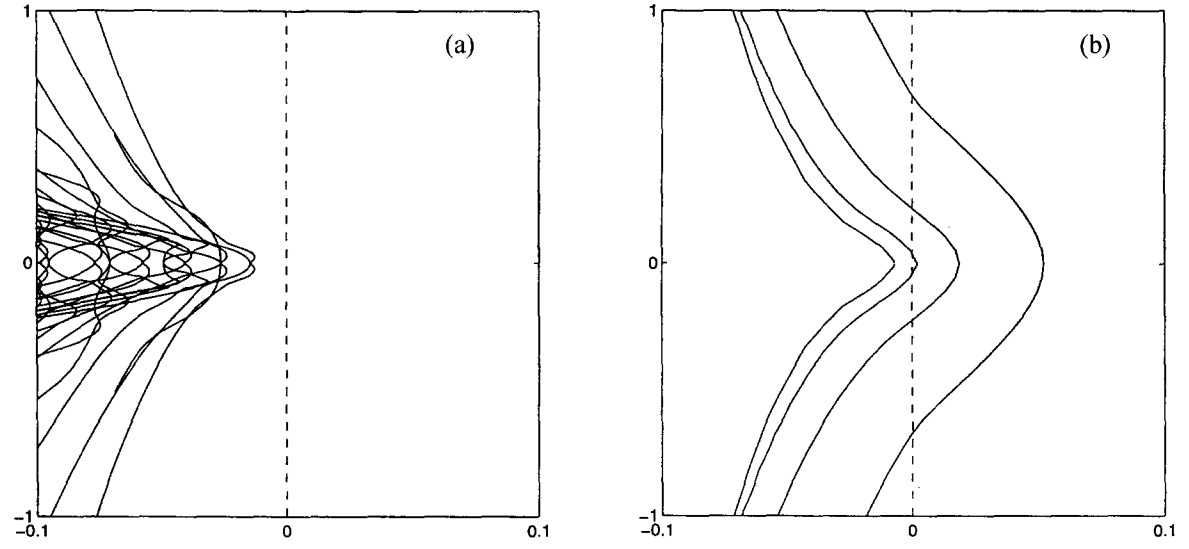

Fig. 1. (a) Spectrum $\Lambda(\mathscr{L})$ for $R = 1000$. (b) Boundaries of ϵ-pseudospectra $\Lambda_\epsilon(\mathscr{L})$ for the same operator (from right to left: $\epsilon = 10^{-2}$, $10^{-2.5}$, 10^{-3}, $10^{-3.5}$). These and other curves in this paper are thought to be correct not to full plotting accuracy, but to within a millimeter or two at each point.

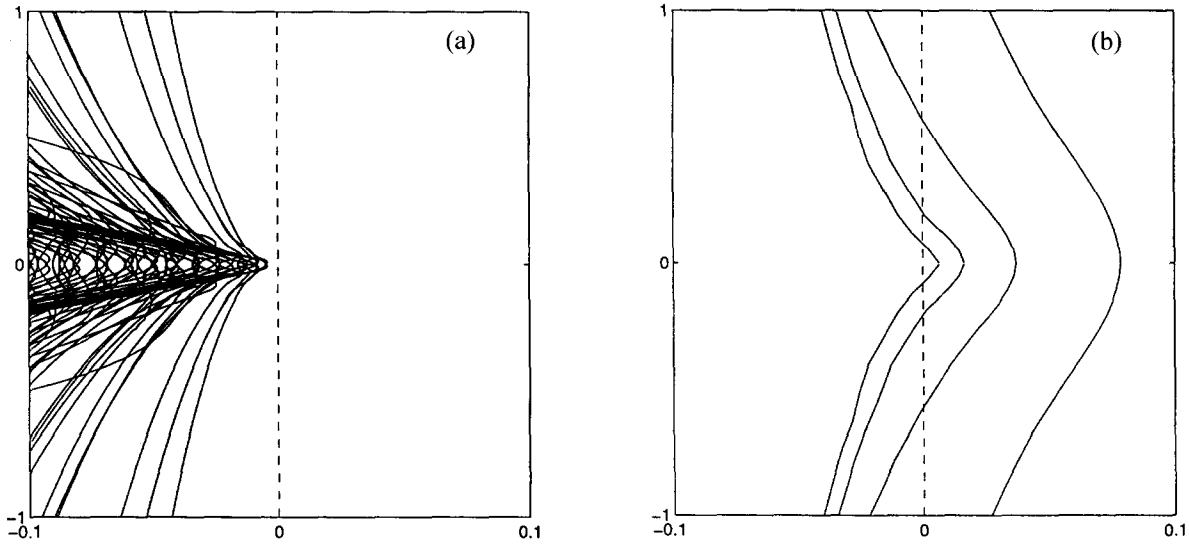

Fig. 2. (a) Spectrum $\Lambda(\mathscr{L})$ for $R = 3000$. (b) Boundaries of ϵ-pseudospectra $\Lambda_\epsilon(\mathscr{L})$ for the same operator ($\epsilon = 10^{-2}$, $10^{-2.5}$, 10^{-3}, $10^{-3.5}$).

Being a collection of curves, the spectrum for pipe Poiseuille flow looks quite different from that for plane Poiseuille or Couette flow, where we get a two-dimensional continuum due to the presence of two continuous Fourier variables [24]. One might think this fundamental difference in the spectra must reflect a fundamental difference in the physics of pipes and channels, but we believe this is not the case, since the overall shapes of the spectra are comparable and the pseudospectra are more important physically anyway.

From Figs. 1(a)–3(a) it appears that the spectrum of $\mathscr{L}$ grows more complicated as R increases. In fact, most of what is happening is a linear scale change,

$$\Lambda(\mathscr{L}^{(\tau R)}) \approx \tau^{-1}\Lambda(\mathscr{L}^{(R)}), \tag{4}$$

where $\mathscr{L}^{(R)}$ denotes the operator $\mathscr{L}$ corresponding to Reynolds number R. In particular, the spectral abscissa decreases to 0 in proportion to R^{-1}: we have approximately

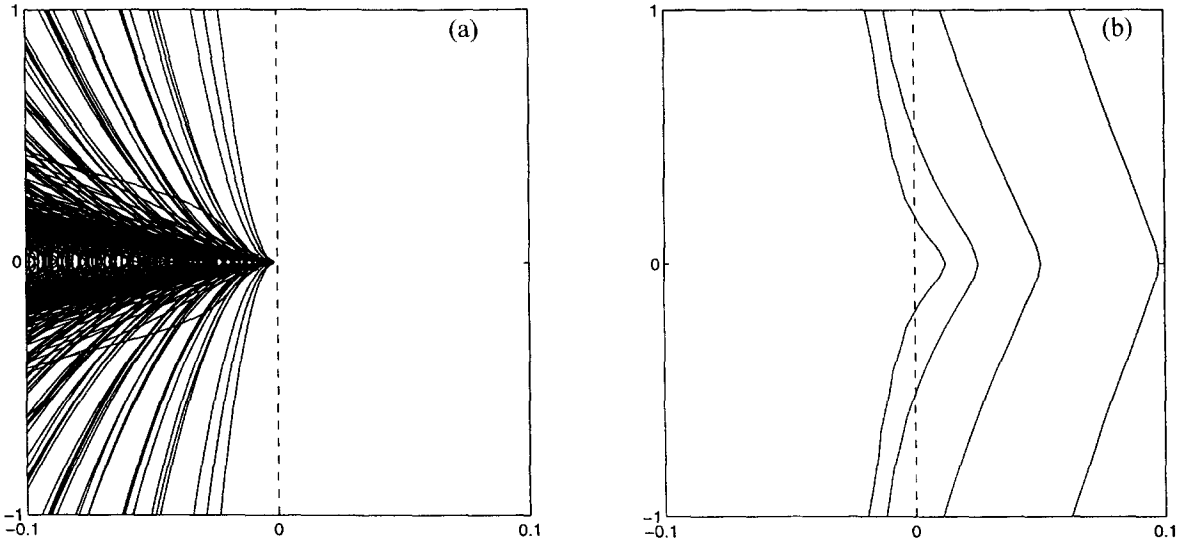

Fig. 3. (a) Spectrum $\Lambda(\mathscr{L})$ for $R = 10\,000$. (b) Boundaries of ϵ-pseudospectra $\Lambda_\epsilon(\mathscr{L})$ for the same operator ($\epsilon = 10^{-2}, 10^{-2.5}, 10^{-3}, 10^{-3.5}$).

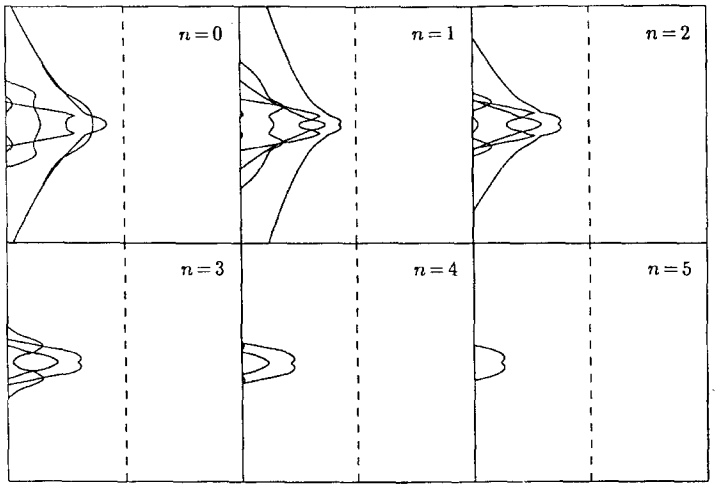

Fig. 4. Breakdown of Fig. 1(a) ($R = 1000$) for various n. The axes are the same as in Figs. 1–3.

$$\max_{\lambda \in \Lambda(\mathscr{L})} \operatorname{Re} \lambda \sim -12.9R^{-1} \tag{5}$$

as $R \to \infty$, with the maximum achieved by a mode with $n = 1$, $\alpha \neq 0$.

In view of the conceptual simplicity of the pipe Poiseuille problem, we find the complexity of Figs. 1(a)–3(a) delightful.

4. Pseudospectra

Figs. 1(b), 2(b) and 3(b) show the boundaries of the ϵ-pseudospectra $\Lambda_\epsilon(\mathscr{L})$ for $R = 1000$, 3000, 10 000 and $\epsilon = 10^{-2}, 10^{-2.5}, 10^{-3}, 10^{-3.5}$. These sets are defined by curves of constant norm of the resolvent,

$$\Lambda_\epsilon(\mathscr{L}) = \{z \in \mathbb{C}: \|(zI - \mathscr{L})^{-1}\| \geq \epsilon^{-1}\}, \tag{6}$$

with the convention that $\|(zI - \mathscr{L})^{-1}\| = \infty$ for $z \in \Lambda(\mathscr{L})$. An equivalent definition is that $\Lambda_\epsilon(\mathscr{L})$ is the set of all points in the complex plane that are eigenvalues of some perturbed operator $\mathscr{L} + \mathscr{E}$ with $\|\mathscr{E}\| \leq \epsilon$. For

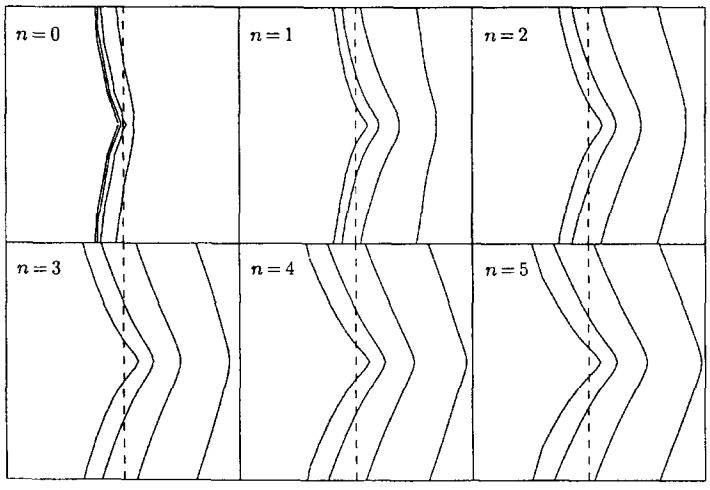

Fig. 5. Breakdown of Fig. 3(b) ($R = 10\,000$) for various n. The axes are the same as in Figs. 1–3.

discussions of the significance of pseudospectra in hydrodynamic stability and in other fields, see [23] and [24].

Visually, the pseudospectra of $\mathscr{L}$ are less striking than the spectra, but physically, they are more important. The important feature is that they extend substantially into the right half-plane—for small ϵ, much further than ϵ. The configuration is much the same as for the plane Poiseuille and Couette flows considered in [24].

Like the spectrum, the pseudospectra of $\mathscr{L}$ are determined by combining results from various n, and again we give a figure to clarify how this works. Fig. 5 shows a breakdown of the case $R = 10\,000$ for $n = 0$, 1, 2, 3. Notice how far from dominant the value $n = 0$ is, corresponding to axisymmetric perturbations of the pipe flow. This axisymmetric part of the operator is relatively close to normal [22] and contributes little to the process of transition to turbulence [4,18]. The value $n = 1$ is dominant for $z \approx 0$, whereas for larger z near the real axis, values of n as great as 6 become dominant.

We noted above that the spectra $\Lambda(\mathscr{L})$ scale approximately with R^{-1}. By contrast, the pseudospectra $\Lambda_\epsilon(\mathscr{L})$ appear to be scale-invariant, approaching fixed limits as $R \to \infty$. From the plots it is natural to guess that in the limit $R \to \infty$, the spectrum of $\mathscr{L}$ is the closed left half-plane and the resolvent set is the open right half-plane, with $\|(zI - \mathscr{L})^{-1}\|$ taking a finite limiting value for each z with $\mathrm{Re}\, z > 0$. At the origin, which is the point of the imaginary axis where the resolvent norm is largest, the growth of $\|(zI - \mathscr{L})^{-1}\|$ with respect to R is quadratic:

$$\|\mathscr{L}^{-1}\| \sim 0.00120R^2 . \tag{7}$$

The maximum is achieved by a (pseudo-) mode with $n = 1$, $\alpha = 0$.

We should mention that Figs. 1(b)–3(b) are not in fact complete depictions of the pseudospectra of $\mathscr{L}$. There are additional components of each pseudospectrum in the left half-plane, between the various curves of the spectrum, which we have not attempted to resolve.

5. Discussion

We shall not attempt to discuss the significance of our computations in detail, referring the reader to [3,4,16,18,22,26] for treatments of linear, non-modal effects in pipe Poiseuille flow and to [23] and [24] for further matters related to pseudospectra. In [24] it is pointed out that pseudospectra may provide insight into three related but distinct forms of destabilization that may apply in different flow situations. First, the interpretation of Figs. 1(b)–3(b) in terms of eigenvalue perturbations suggests that slight perturbations from the ideal of an infinitely long straight pipe, such as irregularities in the boundary wall, may be expected to move some eigenvalues into the right half-plane and thereby bring about modal instabilities. Second, the interpretation in terms of the norm of the resolvent suggests that since the resolvent norm is large at points on the imaginary

axis, substantial 'pseudoresonance' may occur when a pipe flow is stimulated by periodic inputs at certain frequencies. This is the subject of *receptivity*, recently investigated for pipe flows by Tumin [25]. Third is the aspect of non-normal physics that has received the most attention, the phenomenon of transient growth of certain perturbations.

Fig. 6 illustrates transient growth for the pipe problem by depicting $\|e^{t\mathscr{L}}\|$ as a function of t for $R = 10\,000$. The most important feature of this curve is that it achieves a height much greater than 1: about 84.9, attained at $t \approx 490$. Both of these numbers scale in proportion to R. Thus, pipe Poiseuille flow is susceptible to linear, non-modal amplification of disturbances by factors on the order of hundreds for Reynolds numbers of practical interest. If one takes the square of the perturbation amplitude as a measure of energy, then one may speak of energy amplifications by factors of tens of thousands.

The kink in the curve in Fig. 6 at $t = t_c \approx 300$ has a simple explanation. For each fixed n, $\|e^{t\mathscr{L}_n}\|$ depends smoothly on t. The value of $\|e^{t\mathscr{L}}\|$, however, is the upper envelope of these quantities, hence not necessarily smooth. As it happens, for $t > t_c$ the value $n = 1$ is dominant, while for $t < t_c$, larger values of n become dominant. The curve for $t < t_c$ drawn in the figure corresponds to $n = 2$, but in principal there are further kinks near $t = 0$ corresponding to higher values of n. However, these would be scarcely visible on the scale of the plot. For more information see [3,22].

From the pseudospectra of $\mathscr{L}$, upper and lower bounds on this transient growth can be derived. An upper bound would involve a resolvent integral; we do not pursue this here. For a lower bound we can take the maximum over $\epsilon > 0$ of the ratio $\rho_\epsilon(\mathscr{L})/\epsilon$, where $\rho_\epsilon(\mathscr{L})$ denotes the ϵ-pseudospectral abscissa of $\mathscr{L}$, that is, the maximum real part of the ϵ-pseudospectrum. (This bound can be derived from the Laplace transform of e^{tA}; see [19,23,24].) This quantity can be estimated by sampling $\|(zI - \mathscr{L})^{-1}\|$ for z on the positive real axis, and from this we get the lower bound 55.7 plotted as a dashed line in Fig. 6. Like the actual height of the transient growth curve, this bound scales in proportion to R as $R \to \infty$.

Of course, linear transient growth in itself does not constitute turbulence or transition to turbulence, but it must play a part in these phenomena, as the nonlinear terms of the Navier–Stokes equations conserve the energy of perturbations of the laminar flow [12]. The fact that the excited pseudomodes (= left singular vectors of $e^{t\mathscr{L}}$) have the form of streaky structures aligned with the flow, as are seen so often in experiments, adds further weight to the argument. It has been proposed that these linear effects combine with the quadratic nonlinearities of the Navier–Stokes equations in such a way as to produce a very narrow basin of attraction of the laminar state in the state space of all velocity perturbations, and that this accounts for the tendency of at least some pipe flows at high Reynolds numbers to undergo transition [1,2,4,10,24]. This reasoning led to a conjecture stated in [24]: the threshold perturbation amplitude for transition to turbulence decreases superlinearly with R, that is, it is $O(R^\gamma)$ for some $\gamma < -1$ as $R \to \infty$. For channel flows, this conjecture has subsequently been verified by Navier–Stokes simulations of Henningson, Lundbladh and Reddy [11,15]. For pipe Poiseuille flow, no

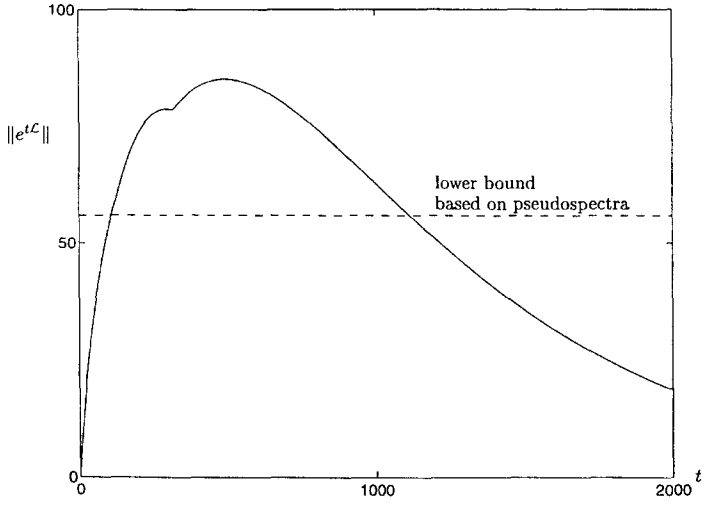

Fig. 6. $\|e^{t\mathscr{L}}\|$ as a function of t for $R = 10\,000$.

analogous simulations have yet been carried out, but exceptionally careful experimental results have recently been reported by Darbyshire and Mullin [7] and Nieuwstadt et al. [17]. Both sets of authors report exponents γ in the range $-1 < \gamma < 0$, but in both cases the definition of perturbation amplitudes differs from the usual energy norm in a nontrivial way. After appropriate correction, the experimental evidence of [7] and [17] may be consistent with $\gamma < -1$ after all, but this issue is not yet resolved.

6. Computational methods

To produce the plots presented here, one must first discretize the operator $\mathscr{L}$. For this purpose we used the codes developed by the third author and described in [22], based on earlier work by Burridge and Drazin [5] and Herbert [13], among others. These codes handle the x and θ variables by Fourier transformation and the r variable by a hybrid spectral collocation method based on Chebyshev polynomials; the dependent variables are the radial velocity and the radial vorticity. For computing pseudospectra and other norm-dependent quantities, the resulting matrices are then modified by a similarity transformation so that the matrix 2-norm becomes the physically correct energy norm $\|\cdot\|$. Further details are given in [22].

Since our aim has been to present plots comprehending all values of α and n, the scale of our computations has been larger than in previous studies. To produce Figs. 1(a)–3(a), we calculated the spectrum of $\mathscr{L}$ for 7–25 values of n and several hundred values of α; each of these spectra is obtained by solving a complex matrix eigenvalue problem of dimension on the order of 50 to 100. Thus, each spectral plot represents several thousand matrix eigenvalue calculations. Figs. 1(b)–3(b) required a greater effort. Here, we evaluate $\|(zI - \mathscr{L})^{-1}\|$ on a grid in the upper half-plane of size approximately 30×30, reflect the result by symmetry into the lower half-plane, and send the result to a contour plotter. Each evaluation of $\|(zI - \mathscr{L})^{-1}\|$ requires optimization over n (discrete, carried out trivially since only half a dozen values are involved) and α (continuous, carried out by a univariate optimization routine). In the end, each plot of pseudospectra represents 10^4–10^5 complex matrix singular value calculations, again with matrix dimensions on the order of 50–100. The total number of floating-point operations for such a plot is on the order of 3×10^{11}.

Some of these computations have been carried out in Matlab on workstations, but for satisfactory performance it is convenient to use faster machines. The bulk of our work has been based on Fortran programs run in 1994 on the Intel Paragon at the Swiss Federal Institute of Technology (ETH) in Zurich. The problem is embarrassingly parallel; we use, typically, 30 processors, each assigned a different value of Im z. A succession of values of Re z are treated on each processor, decreasing from Re $z = 0.1$ until the spectrum is reached, and the optimal Fourier parameter α obtained in the minimization for each value of z is utilized as an upper limit on α for the minimization at the next value of z; the lower limit is taken as Re z. The computational kernels are based on LAPACK routines on the Paragon, and the overall computation speeds we obtain are typically on the order of one third of a gigaflop when running on 30 processors, or one gigaflop when running with a finer grid on the full 96 processors available at the ETH. These figures could certainly be improved, as we made no attempt to optimize the code for performance on the Paragon.

We close with a remark about the accuracy of our plots. The discretizations we employ are spectrally accurate; they reliably provide three or four digits of precision with matrices of dimension <100, and higher precision does not cost much more. Thus, accuracy is not fundamentally an issue in our computations. However, grid resolution is an issue when it comes to plotting pseudospectra, and our grids are not as fine as they might have been. This explains the slight irregularities apparent in some of the plots: our data are effectively exact, but they are coarsely sampled. We are confident that all the points on our curves are correct to within a millimeter or two.

Acknowledgments

LNT has been supported by U.S. NSF Grant DMS-9500975CS, and PJS by the Deutsche Forschungsgemeinschaft (DFG). The work of AET and LNT was performed during a visit in the summer of 1994 to the Interdisziplinäres Projektzentrum für Supercomputing at the Swiss Federal Institute of Technology in Zurich. We wish to extend our thanks to the IPS and to its director, Martin Gutknecht, for supporting our visit and for providing excellent facilities and a stimulating research environment.

References

[1] J.S. Baggett, T.A. Driscoll and L.N. Trefethen, A mostly linear model of transition to turbulence, Phys. Fluids 7 (1995) 833–838.
[2] J.S. Baggett and L.N. Trefethen, Low-dimensional models of subcritical transition to turbulence, Phys. Fluids 9 (1997) 1043–1053.
[3] L. Begström, Optimal growth of small disturbances in pipe Poiseuille flow', Phys. Fluids A 5 (1993) 2710–2720.
[4] L. Boberg and U. Brosa, Onset of turbulence in a pipe, Z. Naturforschung 43a (1988) 697–726.
[5] D.M. Burridge and P.G. Drazin, Comments on 'Stability of pipe Poiseuille flow, Phys. Fluids 12 (1969) 264–265.
[6] K.M. Butler and B.F. Farrell, Three-dimensional optimal perturbations in viscous shear flow, Phys. Fluids A 4 (1992) 1637–1650.
[7] A.G. Darbyshire and T. Mullin, Transition to turbulence in constant-mass-flux pipe flow, J. Fluid Mech. 289 (1995) 83–114.
[8] A. Davey and P.G. Drazin, The stability of Poiseuille flow in a pipe, J. Fluid Mech. 36 (1969) 209–218.
[9] P.G. Drazin and W.H. Reid, Hydrodynamic Stability (Cambridge University Press, Cambridge, 1981).
[10] T. Gebhardt and S. Grossmann, Chaos transition despite linear stability, Phys. Rev. E 50 (1994) 3705–3711.
[11] D.S. Henningson, Bypass transition and linear growth mechanisms, in: R. Benzi, ed., Advances in Turbulence V (Kluwer, 1995).
[12] D.S. Hennington and S.C. Reddy, On the role of linear mechanisms in transition to turbulence, Phys. Fluids 6 (1994) 1396–1398.
[13] T. Herbert, Die neutrale Fläche der ebenen Poiseuille Strömung, Habilitationschrift, Universität Stuttgart, 1977.
[14] I. Herron, The linear stability of circular pipe flow to axisymmetric disturbances, Stab. Appl. Anal. Continuous Media 2 (1992) 293–303.
[15] A. Lundbladh, D.S. Henningson and S.C. Reddy, Threshold amplitudes for transition in channel flows, in: Transition, Turbulence, and Combustion, Vol. 1 (Kluwer, 1994).
[16] E.W. Mayer and E. Reshotko, Evidence for transient disturbance growth in a 1961 pipe-flow experiment, Phys. Fluids 9 (1997) 242–244.
[17] F.T.M. Nieuwstadt, A.A. Draad and G.D.C. Kuiken, Laminar-turbulent transition in pipe flow, in: S. Gavrilakis et al., eds., Advances in Turbulence VI (Kluwer, 1996) 371–374.
[18] P. O'Sullivan and K. Breuer, Transient growth in circular pipe flow. Part I: linear disturbances, Phys. Fluids 6 (1994) 3643–3651.
[19] S.C. Reddy and D.S. Henningson, Energy growth in viscous channel flows, J. Fluid Mech. 252 (1993) 209–238.
[20] O. Reynolds, An experimental investigation of the circumstances which determine whether the motion of water shall be direct or sinuous, and of the law of resistance in parallel channels, Phil. Trans. Roy. Soc. 174 (1883) 935–982.
[21] H. Salwen, F.W. Cotton and C.E. Grosch, Linear stability of Poiseuille flow in a circular pipe, J. Fluid Mech. 98 (1980), 273–284.
[22] P.J. Schmid and D.S. Henningson, Optimal energy density growth in Hagen–Poiseuille flow, J. Fluid Mech. 277 (1994) 197–225.
[23] L.N. Trefethen, Pseudospectra of linear operators, SIAM Rev. 39 (1997) 383–406.
[24] L.N. Trefethen, A.E. Trefethen, S.C. Reddy and T.A. Driscoll, Hydrodynamic stability without eigenvalues, Science 261 (1993) 578–584.
[25] A. Tumin, Receptivity of pipe Poiseuille flow, J. Fluid Mech. 315 (1996) 119–137.
[26] O. Zikanov, On the instability of pipe Poiseuille flow, Phys. Fluids 8 (1996) 2923–2932.